Canadian Chemical Transactions Year 2016 | Volume 4 | Issue 2 | Page 244-254

Research Article

DOI:10.13179/canchemtrans.2016.04.02.0299

Effect of Temperatures on Structural, Morphological and Magnetic Properties of Zinc Ferrite Nanoparticles

P. Sivagurunathan* and K. Sathiyamurthy

Department of Physics, Annamalai University, Annamalainagar 608 002, India

**Corresponding Author, Email: sivagurunathanp2012@yahoo.com*

Received: *April 4, 2016* ***Revised:*** *May 28, 2016* ***Accepted:*** *June 6, 2016* ***Published:*** *June 8, 2016*

Abstract: Zinc ferrite ($ZnFe_2O_4$) nanoparticles have been synthesized by co-precipitation method with citrate as chelating agent. The as-prepared sample was characterized by thermo gravimetric and differential thermal analysis. The synthesized materials were annealed at different temperatures, such as 400 °C, 600 °C and 800 °C and the product was characterized by using XRD, FTIR and VSM. $ZnFe_2O_4$ nanoparticles annealed at 600 °C were phase pure, which is further characterized by FESEM with EDAX and FETEM with SAED pattern. XRD results reveals the formation of single phase nano sized zinc ferrite, also the particle size and the X-ray density of the annealed $ZnFe_2O_4$ nanoparticles linearly increased with increase in temperature and decrease in lattice parameters were noticed. FTIR study confirms the presence of zinc ferrite nanoparticles. The surface morphology of $ZnFe_2O_4$ observed by FESEM, which showed that the $ZnFe_2O_4$ nanoparticles annealed at 600 °C possess spherical structure, which was well supported by FETEM results. The composition of elements Fe, Zn and O in the $ZnFe_2O_4$ nanoparticles were identified by using EDAX spectra. A VSM result of the $ZnFe_2O_4$ nanoparticles reveals the decrease of magnetization by increasing the annealing temperature.

Keywords: Nanoparticles, Characterized, Annealing, Magnetic properties.

1. INTRODUCTION

Ferrites are the most extensively superior magnetic materials than pure metals due to their reasonable cost, high resistivity remarkable magnetic properties, easiness of preparation and better mechanical strength. Zinc ferrite ($ZnFe_2O_4$) nanoparticles have attracted in recent days due to their high magnetic permeability, non-toxicity, low eddy current loss, excellent phase stability, high electronic conductivity and their low cost [1]. Zinc ferrite is a spinel structure where Zn^{2+} ions are occupied at "A" site namely tetrahedral site and Fe^{3+} ions are accommodated at "B" site namely octahedral site [2]. The preparation of spinel $ZnFe_2O_4$ nanoparticles has been intensively studied in the recent years and the major role of the synthesize condition on the morphological and structural features of the ferrites is discussed. $ZnFe_2O_4$ nanoparticles are used in many fields for example high density magnetic storage, radar absorbent materials, hot gas desulphurization, photo catalysis and drug delivery system [3-7]. $ZnFe_2O_4$ nanoparticles are prepared by numerous methods, such as sol-gel, hydrothermal, electrochemical, wet high energy ball milling, thermal treatment, solvothermal and co-precipitation method [8-14]. Among the others, the co-

precipitation method is the most suitable method for the present work for their high efficiency, low reaction temperatures, and environmentally friendliness. In the present work, an attempt has been made to synthesize $ZnFe_2O_4$ nanoparticles by employing co-precipitation method. The synthesized sample was annealed at three different temperatures namely 400 °C, 600 °C and 800 °C. The structural, morphological, thermal and magnetic studies of annealed samples were characterized by using the techniques XRD, FTIR, FESEM, FETEM, TG-DTA and VSM.

2. Materials and methods

$ZnFe_2O_4$ nanoparticles were synthesized by adopting simple co-precipitation method with citrate as a chelating agent [15]. For the synthesis of zinc ferrite nanoparticles, Zn $(NO_3)_2.6H_2O$, Fe $(NO_3)_3.9H_2O$, $C_6H_8O_7$, sodium hydroxide, hydrochloric acid and acetone were used. All the chemicals used in the research experiment were purchased from Merck (AR grade) chemicals with 99% purity and used without any further purification. A synthesis procedure step wise description of $ZnFe_2O_4$ fine particles is shown in Fig.1.

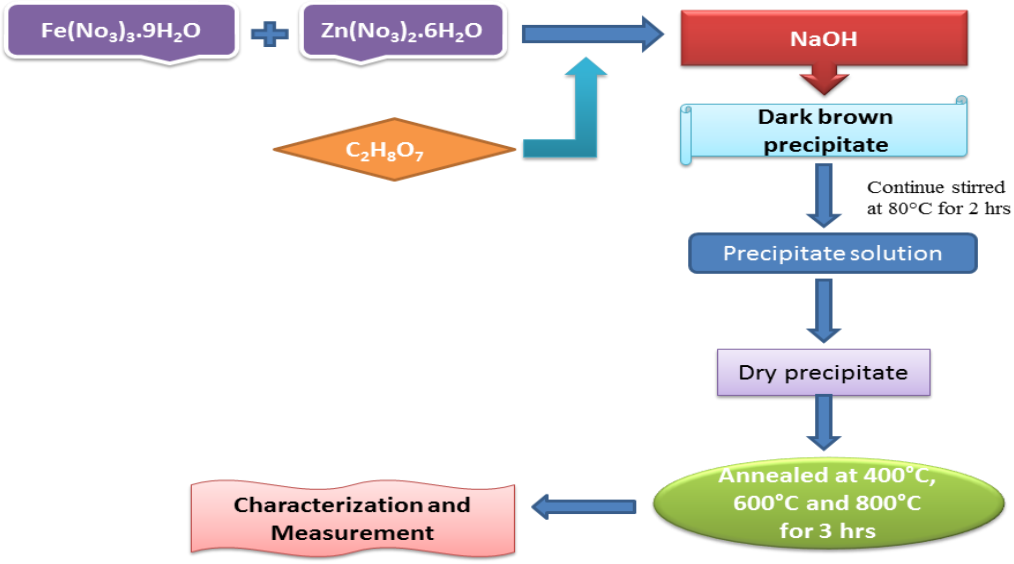

Figure 1. Flow chart showing the synthesis of $ZnFe_2O_4$ nanoparticles

So as to synthesize $ZnFe_2O_4$ nanoparticles, 3.23g of Iron (iii) nitrate nonahydrate[Fe $(NO_3)_3.9H_2O$] and 1.18g of zinc nitrate hexahydrate [Zn $(NO_3)_2.6H_2O$] were dissolved in 20 ml of distilled water respectively. Followed by drop by drop addition of 2.3g of citric acid ($C_6H_8O_7$) to the nitrate solution under constantly stirred. The pH value of the nitrate solution was maintained at 8, by adding the required amount of sodium hydroxide (NaOH) solution dropwise as a precipitate agent. The solution was then kept at 80 °C for 120 min. This duration was sufficient for the formation of hydroxides into spinel ferrite. The precipitate was washed out by magnetic decantation with distilled water and acetone to remove the impurities. The product was dried in an electric oven at 70 °C temperature for two hours. Finally, the dried powder was then, ground using an agate field gun to obtain very fine particles and was annealed at 400 °C, 600 °C and 800 °C for 3 h.

2.1 Characterization Techniques

The composition and crystalline structure of the zinc ferrite nanoparticles were analyzed by PW3040/60 XPERT-PRO prefix X-ray diffractometer using monochromatic CuK_{α} radiation (λ= 1.5405 Å). XRD pattern was recorded in the range of 20° to 80°. The average particle size of the samples was calculated by applying peak expansion of (311) line of cubic spinal structure using Debye-Scherer formula [16]

$$D = \frac{0.9\lambda}{\beta \cos\theta} \qquad (1)$$

Where D is mean crystallite size, K (= 0.9) is a constant to the shape of the crystal, λ is wavelength of radiated X-ray (in Å), θ is corresponds to Bragg diffraction angle at the peak position and β is fullwidth at half maximum intensity measured in radians. Thermal analysis was used to study of change in properties of the sample with temperature. The TG/DTA analysis was carried out using the instrument NETZSCH - STA 449 F3 JUPITER. FTIR spectra analyses were carried out on samples pelletized using KBr powder in the region between 1000 cm^{-1} and 400 cm^{-1} using a Tensor 27 BURKER. FESEM with EDAX was recorded using a model ZEISS SUPRA 40 VP SEM. FETEM system which has been used for morphology and size determination was achieved using a FETEM instrument model JEOL JEM-2100F. The SAED patterns were confirmed by dispersing the sample in excess of a carbon coated copper grid. Using the instrument VSM lakeshore-7404, magnetic measurements were carried out at room temperature up to a maximum field of 15 kOe.

3. Results and Discussion

3.1 Structural properties

The structure of synthesized product was identified by powder XRD method. The XRD patterns of the as-synthesized and annealed at 400 °C, 600 °C and 800 °C of zinc ferrite nanoparticles are shown in Fig.2.

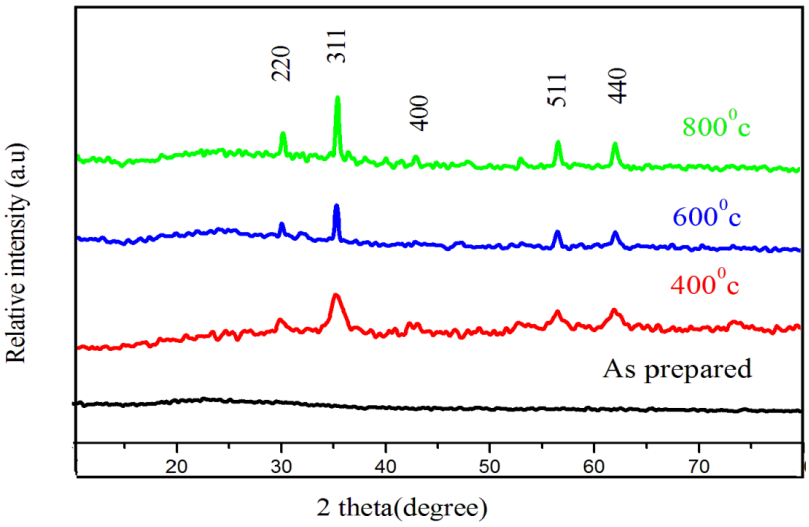

Figure 2. XRD Spectra of $ZnFe_2O_4$ nanoparticles as-synthesized and annealed at different temperatures

All the samples are exhibiting the diffraction peaks of 29.3°, 35.2°, 42.5°, 56.1° and 62.1°. The observed peaks are compared with ICDD PDF: 22-1012 and concluded that the synthesized product is single phase cubic zinc ferrite nanoparticles. No additional peak is observed in the XRD pattern, and it confirms that the synthesized product is zinc ferrite nanoparticles and free from any impurities. Similar result was reported by Raeisi Shahraki et. al.,[17] for synthesized zinc ferrite nanoparticles. The average particle size is calculated from the width of the prominent peak (311) using Scherer's equation as shown in table 1.

Table 1 particle size D (nm), lattice parameter 'a' (Å), X-ray density (d_x), Saturation magnetization (M_s) and Coercivity (H_c) value of $ZnFe_2O_4$ nanoparticles annealed at 400 °C, 600 °C and 800 °C .

material	Annealing temperature °C	D (nm)	a (nm)	d_x (gm/cm^3)	M_s emu/g	H_c (O_e)
$ZnFe_2O_4$	400°C	8	8.465	5.279	24.013	84.957
	600°C	11	8.464	5.282	20.347	9.314
	800°C	38	8.453	5.302	4.774	0.296

The lattice parameter 'a' can be calculated using the relation

$$a = d\,(h^2+k^2+l^2)^{1/2} \qquad (2)$$

Where `a` is the lattice parameter, d represents the interplanar spacing, and h, k, and l indicate the Miller indices. The interplanar spacing d can be calculated by using the eminent Bragg law. From our investigations we observed that the particle size increases with the lattice parameter continues to decrease. The X-ray density (d_x) values are calculated from the XRD data using this relation was observed by Smit and Wijn [18]

$$d_x = ZM / Na^3 \qquad (3)$$

Where d_x is the X-rays density (g/cm^3), Z = 8 spinel cubic structure corresponds to the number of molecules in a unit cell of spin lattice, M is the molecular weight of the samples, N_a indicates the Avogadro's number, and "a" represents the lattice parameter. From the table 1, it is clear that the particle size and X-ray density (d_x) are increased with increasing annealed temperatures from 400 °C to 600 °C, 600 °C to 800 °C, whereas decrease the lattice parameter ('a') with increasing annealed temperatures. Similar result was reported by Rintu Mary Sebastian et. al.,[19] for the preparation of zinc ferrite nanoparticles at different temperatures.

3.2 Thermal analysis

Thermal stability of the synthesized $ZnFe_2O_4$ nanoparticles was examined by simultaneous TG and DTA measurement. The result was carried out from room temperature to 850 °C temperatures at a heating rate of 10°C/min which is shown in Fig.3.

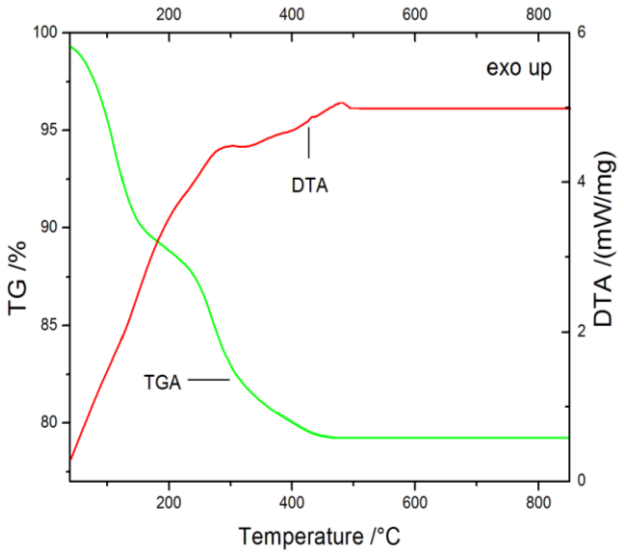

Figure 3. TG–DTA curve of $ZnFe_2O_4$ nanoparticles

Three major weight losses have been found from TG analysis. The first stage of weight loss is observed at a temperature below 83 °C (2%) due to desorption of water. The second weight loss is predicted in the range from 84 °C to 235 °C (10%) as a result of decomposition of organic templates. The third weight loss of (9%) is observed between 236 °C and 460 °C due to crystallization of the final product. No weight loss is found beyond 460 °C indicating the formation of $ZnFe_2O_4$ nanoparticles. There are two broad exothermic peaks observed in DTA curve at 290 °C and 440 °C. The first broad exothermic peak in DTA curve at 290 °C due to the thermal decomposition of citric acid. The second exothermic peak at 440 °C corresponds to the formation of intermediate phases, which is associated in the formation of $ZnFe_2O_4$ nanoparticles. Similar result was reported by Yang *et. al*., [20] for the synthesis of zinc ferrite nanopowders.

3.3 FTIR studies

FTIR spectra of zinc ferrite nanoparticles annealed at 400 °C, 600 °C and 800 °C are shown in Fig.4 in the region of 1000 to 400 cm^{-1}.

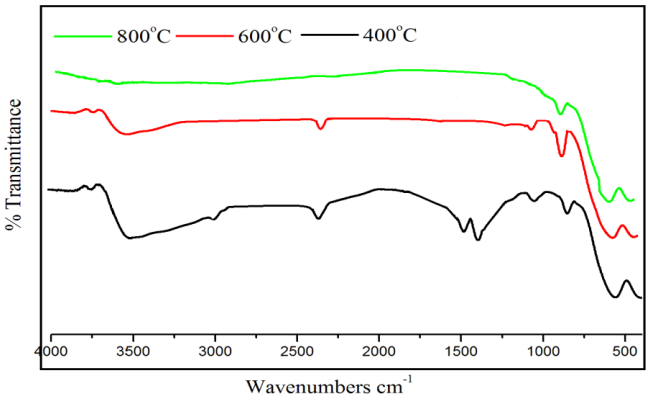

Fig. 4 FTIR spectra of $ZnFe_2O_4$ nanoparticles annealed at different temperatures

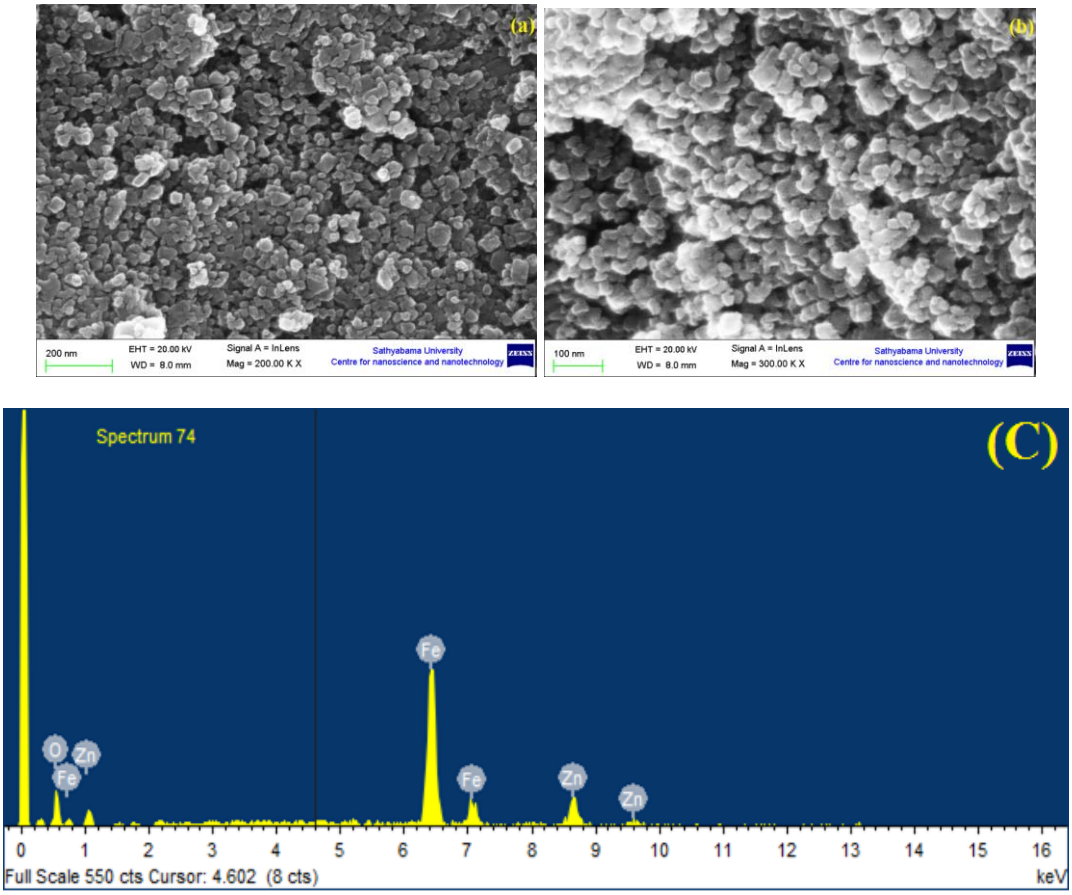

Figure 5. FESEM image of $ZnFe_2O_4$ nanoparticles annealed at 600 °C with different magnifications (a), (b) (c) matching EDAX

All samples exhibited the peaks near 550 cm^{-1}corresponding to the Fe-O stretching vibration and peaks near 425 cm^{-1} is ascribed due to the stretching modes of Zn-O [21]. From this study it may be concluded that the observed peaks are the characteristic peaks of zinc ferrite nanoparticles. The absorption bands Fe-O are observed at 550, 553, and 557cm^{-1} and the absorption band Zn-O are observed at 425, 429, and 434 cm^{-1} for the zinc ferrite nanoparticles annealed at 400 °C, 600 °C and 800 °C respectively is shown in table 2. The samples were annealed at high temperature all the other bands are disappeared and the zinc ferrite gorge shifts towards lower frequency.

Table 2 FTIR absorption bands of $ZnFe_2O_4$ nanoparticles annealed at 400 °C, 600 °C and 800 °C.

Samples	400°C		600°C		800°C	
	V_1 (cm^{-1})	v_2 (cm^{-1})	V_1 (cm^{-1})	v_2 (cm^{-1})	V_1 (cm^{-1})	v_2 (cm^{-1})
$ZnFe_2O_4$	550	425	553	429	557	434

The shifting of absorption band at higher frequency in the present study clearly suggest that the linear relationship between the particle size and annealing temperatures. Similar trend was observed by IsrafUd Din *et.al*., [22] for synthesize of zinc ferrite nanoparticles. This observation from the FTIR study strongly support the result observed by XRD study.

3.4 FESEM with EDAX

Shape and size of the synthesized $ZnFe_2O_4$ nanoparticles were characterized by FESEM measurements. From The morphology of $ZnFe_2O_4$ nanoparticles annealed at 600 °C investigated by FESEM is shown in Fig.5 (a, b).

The observed FESEM shows that the synthesized zinc ferrite nanoparticles are spherical in shape. Similar result was observed by Panit Chantharasupawong *et.al*.,[23] for synthesized zinc ferrite nanoparticles. The EDAX spectrum and quantitative results of zinc ferrite nanoparticles are shown in Fig.5 (c). From EDAX spectrum, the presence of Zn, Fe and O are observed with atomic percentages of 19.30%, 52.87% and 27.83% respectively. No additional compounds are observed in the present study which confirms the $ZnFe_2O_4$ nanoparticles are free from impurities. Similar result was drawn by Rameshbabu *et.al*.,[24] for synthesized zinc ferrite nanoparticles. The observed result from EDAX is in close agreement with the XRD study.

3.5 FETEM with SAED

FETEM provides further insight into the morphologies and structural details of these samples. Fig. 6(a, b, c) shows the FETEM images annealed at 600°C with different scale bar which confirms the clear morphology of $ZnFe_2O_4$ nanoparticles.

The observed FETEM pattern confirms that the synthesized sample is zinc ferrite nanoparticles with agglomerated spherical shape. These agglomerates can be able to increase the magnetic interaction between the particles, and then might influenced the magnetic properties of $ZnFe_2O_4$ nanoparticles [25]. From the FETEM image the average particle size 12.5 nm was measured to image j viewer software [26] be which is shown in Fig.6 (c). The selected area electron diffraction (SAED) pattern of the spherical shaped $ZnFe_2O_4$ Nanoparticles is shown in Fig. 6(d). All spots are identified with the diffractions pattern of spherical, which reveals the crystalline nature of zinc ferrite Nanoparticles. The single-phase zinc ferrite Nanoparticles observed from SAED pattern is in good agreement with FESEM result. Similar result was observed by Gharagozlou *et.al*.,[27] for synthesized zinc ferrite nanoparticles.

3.6 Magnetization studies

Magnetization as a function of applied magnetic field at different temperatures of annealed zinc ferrite nanoparticles is shown in Fig.7.

The saturation magnetization (Ms) and coercivity (Hc) of zinc ferrite nanoparticles annealed at different temperature values are provided in table 1. The saturation magnetization and coercivity value decreased with increasing annealed temperatures are observed. The result observed in the present study is in close agreement with Sushant Singh *et.al*.,[28] for the preparation of zinc ferrite nanoparticles. The coercivity value is near to zero observed at 800 °C reflects the super paramagnetic behavior of $ZnFe_2O_4$ nanoparticles. Similar result was reported by Yan Xu et. al.,[29] for the synthesized zinc ferrite nanoparticles by sol-gel method. The magnetizations of the samples at 400 °C, 600 °C and 800 °C evaluated by extrapolating the high field magnetization curve are found to be values are 24, 20, and 4

emu/g respectively, which are larger than the zinc ferrite nanoparticles prepared by other methods [30, 31]. From the M–H curves, as the annealing temperature were increased from 400 °C to 600 °C and 600 °C to 800 °C, a transition from paramagnetic to ferromagnetic region was observed in zinc ferrite nanoparticles. This transition is attributed to the partial inversion of zinc and ferric ions in tetrahedral and octahedral sites respectively. The comparison between magnetizations of 400 °C, 600 °C and 800 °C samples shows decrease of the surface cation disordering due to increase in particle size and crystallinity accompanied cation redistribution in decreasing magnetization [31].

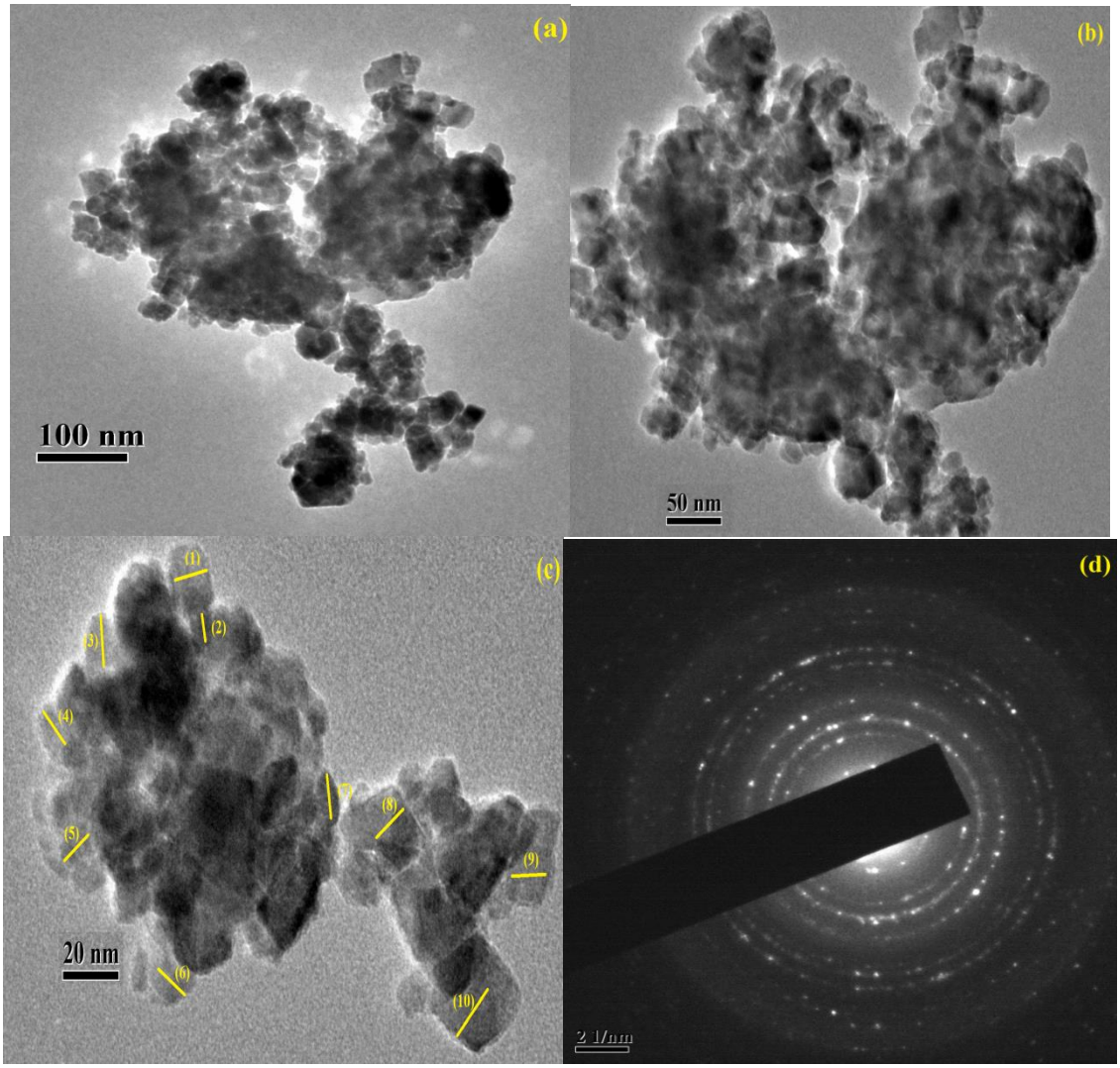

Figure 6. FETEM of $ZnFe_2O_4$ nanoparticles annealed at 600 °C with different magnification (a), (b) and (c) Particle size measured using image viewer software (d) resultant SAED

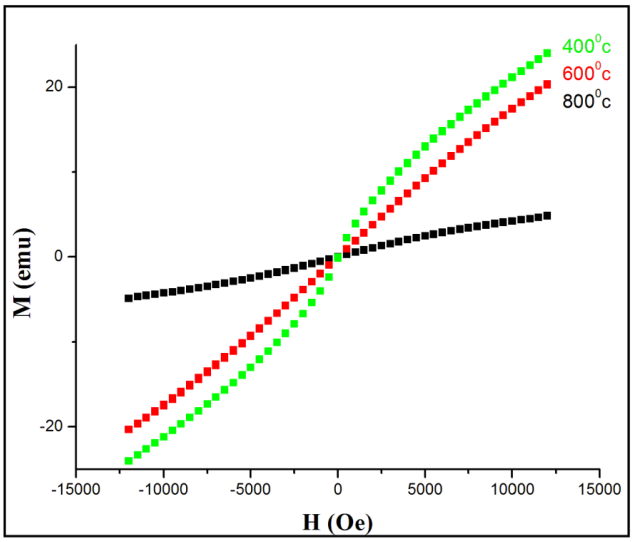

Figure 7. Room temperature M-H curves for $ZnFe_2O_4$ nanoparticles annealed at 400 °C, 600 °C and 800 °C.

4. CONCLUSION

$ZnFe_2O_4$ nanoparticles were successfully prepared by a simple, high yield and low cost co-precipitation method. Structural, compositional and magnetic properties of the synthesized $ZnFe_2O_4$ nanoparticles at different annealing temperatures were well studied. XRD study reveals that the synthesized $ZnFe_2O_4$ nanoparticles were of phase pure with cubic structure. Particle size and X-ray density gets increased with increase in annealing temperature, whereas the decreasing trend was observed in the lattice parameter values. The particle size calculated from Debye-Scherer method in XRD well matches with the particle size calculated by using image j viewer software in FETEM analysis .No weight losses were noticed from 460 °C in TGA and from 440 °C in DTA study confirmed the formation of $ZnFe_2O_4$ nanoparticles. FTIR confirmed the presence of zinc ferrite nanoparticles at all annealing temperatures and the characteristic absorption bands increase with the increase in particle sizes were also noticed which is supported by XRD study. Morphological study of FESEM and FETEM images reveals that the particles were in spherical shape. EDAX spectra confirmed the elemental composition of Fe, Zn and O in the synthesized $ZnFe_2O_4$ nanoparticles. The change in magnetization observed in the magnetic properties suggested that $ZnFe_2O_4$ nanoparticles could be very useful in fabricating new magnetic materials.

REFERENCES

[1] Lucas W Yeary, Ji-Won Moon, Claudia J Rawn, Lonnie J Love, Adam J Rondinone, James R. Thompson, Bryan C Chakoumakos, Tommy J Phelps. Magnetic properties of bio-synthesized zinc ferrite Nanoparticles. *J. Magn. Magn. Mater.* **2011**, *32*, 3043–3048.

[2] Kamazawa, K.; Tsunoda, Y.; Odaka, K.; Kohn, K. Spin liquid state in $ZnFe_2O_4$. *J. Phys. Chem. Solids.* **1999**, *60*, 1261.

[3] Andreas Moser, Kentaro Takano, David T Margulies,Manfred Albrecht, Yoshiaki Sonobe, Yoshihiro Ikeda, Shouheng Sunand, Eric E Fullerton. Magnetic recording: advancing into the future. *J. Phys. D: Appl. Phys.* **2002**, *35*, R157–R167.

[4] Che, R. C.; Peng, L. M.; Duan, X. F.; Chen, Q.; Liang, X. L. Microwave Absorption Enhancement and Complex Permittivity and Permeability of Fe Encapsulated within Carbon Nanotubes. *Adv. Mater.* **2004**, *16*, 401-405.

[5] Makoto Kobayashi, Hiromi Shirai, Makoto Nunokawa. Estimation of Multiple-Cycle Desulfurization Performance for Extremely Low-Concentration Sulfur Removal with Sorbent Containing, Zinc Ferrite Silicon Dioxide Composite Powder. *Energy & Fuels*, **2002**, *16*, 1378 -1386.

[6] Yuanyuan Sun, Wenzhong Wang, Ling Zhang, Songmei Sun, Erping Gao. Magnetic $ZnFe_2O_4$ octahedra: Synthesis and visible light induced photocatalytic activities. *Mater. Lett.* **2013**, *98*, 124-127.

[7] Xiaoqiang Yang, Hao Hong, Jamison J Grailer, Ia. Rowland, Alireza Javadi, Samuel A Hurley, Yuling Xiao, Yunan Yang, Yin Zhang, Robert J Nickles, Weibo Cai, Douglas A Steeber, Shaoqin Gong. cRGD-functionalized, DOX-conjugated, and ^{64}Cu-labeled superparamagnetic iron oxide nanoparticles for targeted anticancer drug delivery and PET/MR imaging. *Biomaterials*, **2011**, *32*, 4151-4160.

[8] Petrova, E.; Kotsikau, D.; Pankov, V. Structural characterization and magnetic properties of sol–gel derived $Zn_xFe_{3-x}O_4$ nanoparticles. *J. Magn. Magn. Mater.* **2015**, *378*, 429-435.

[9] Yu, S. H.; Fujino, T.; Yoshimura, M. Hydrothermal synthesis of $ZnFe_2O_4$ ultrafine particles with high magnetization. *J. Magn. Magn. Mater.* **2003**, *256*, 420-424.

[10] María Rivero, Adolfo del Campo, Álvaro Mayoral, Eva Mazario, Jorge Sánchez-Marcos, Alexandra Muñoz-Bonilla. Synthesis and structural characterization of $Zn_xFe_{3-x}O_4$ ferrite nanoparticles obtained by an electrochemical method**.** *RSC Adv.* **2016**, *6*, 40067-40076.

[11] Lemine, O. M.; Bououdina, M.; Sajieddin, M.; Al-Saie, A. M.; Sha, M.; Khatab, A.; Al-hilal, M.; Henini, M. Synthesis, structural, magnetic and optical properties of nanocrystalline $ZnFe_2O_4$. *Physica B*, **2011**, *406*, 1989-1994.

[12] Mahmoud Goodarz Naseri, Elias B. Saiona, Mansor Hashima, Abdul Halim Shaari, Hossein Abasstabar Ahangar. Synthesis and characterization of zinc ferrite nanoparticles by a thermal treatment method. *Solid State Commun.* **2011**, *151*, 1031-1035.

[13] Sireenart Surinwonga, Apinpus Rujiwatrab. Ultrasonic cavitation assisted solvothermal synthesis of superparamagnetic zinc ferrite Nanoparticles. *Particuology*, **2013**, *11*, 588-593.

[14] Kundu, A.; Upadhyay, C.; Verma, H. Magnetic properties of a partially inverted zinc ferrite synthesized by a new coprecipitation technique using urea. *Phys. Lett. A.* **2003**, *311*, 410-415.

[15] Mendonç, E. C.; Jesus, C. B. R.; Folly, W. S. D.; Meneses, C. T.; Duque, J. G. S. Size Effects on the Magnetic Properties of $ZnFe_2O_4$ Nanoparticles. *J. Supercond. Nov. Magn.* **2013**, *26*, 2329-2331.

[16] Jenkins, R.; Snyder, R. L. Introduction to X-ray Powder Diffractometry, John Wiley and Sons Inc., New York. 1996.

[17] Raeisi Shahraki, R.; Ebrahimi, M.; Seyyed Ebrahimi, S. A.; Masoudpanah, S. M. Structural characterization and magnetic properties of superparamagnetic zinc ferrite nanoparticles synthesized by the coprecipitation method. *J. Magn. Magn. Mater.* **2012**, *324*, 3762-3765.

[18] Smi, J.; Wijn, H. P. J. Ferrites. Philips Technical Library, Eind-hoven, 1959.

[19] Rintu Mary Sebastian, Sheena Xavier, Mohammed, E. M. Effect of Sintering Temperature on the Structural Magnetic and Electrical Properties of Zinc Ferrite Samples. *J. Nanomate. Mol. Nanotechnol.* **2015**, *4*, 2.

[20] Yang, J. M.; Yen, F. S. Evolution of intermediate phases in the synthesis of zinc ferrite nanopowders prepared by the tartrate precursor method. *J. Alloy. Compd.* **2008**, *450*, 387-394.

[21] Rao, S.; Rao, C. N. R.; Ferraro, J. R. Infrared and Electronic Spectra of Rare Earth Perovskites: Ortho-Chromites, -Manganites and –Ferrites. *Appl. Spectrosc.* **1970**, *24*, 436.

[22] Israf d Din, S.; Tasleem, A.; Naeem, S.; Maizatul Shaharun, M. J.; Ghassan Al Kaisy. Zinc Ferrite Nanoparticle Synthesis and Characterization; Effects of Annealing Temperature on the Size of Nanoparticles. *Aust. J. basic. Appl. sci.* **2013**, *7(4)*, 154-162.

[23] Panit Chantharasupawong, Reji Philip, Tamio Endo, Jayan Thomas. Enhanced optical limiting in nanosized mixed zinc ferrites. *Appl. Phys. Lett.* **2012**, *100*, 221108.

[24] Rameshbabu, R.; Ramesh, R.; Kanagesan, S.; Karthigeyan, A.; Ponnusamy, S. Structural, morphological and magnetic properties of hydrothermally synthesized $ZnFe_2O_4$ nanoparticles. *J. Mater. Sci. Mater. Electron.* **2014**, *25*, 2583-2588.

[25] Fashen, Li.; Haibo Wang, Li Wang, Jianbo Wang. Magnetic properties of $ZnFe_2O_4$ nanoparticles produced by a low-temperature solid-state reaction method. *J. Magn. Magn. Mater.* **2007**, *309*, 295-299.

[26] Sivagurunathan, P.; Gibin, S. R. Preparation and characterization of nickel ferrite nano particles by co-precipitation method with citrate as chelating agent. *J Mater Sci: Mater Electron.* **2016**, *27(3)*, 2601-2607.

[27] Gharagozlou, M.; Bayati, R. Low temperature processing and magnetic properties of zinc ferrite Nanoparticles. *Superlattices and Microstruct.* **2015**, *78*, 190-200.

[28] Sushant Singh, Naresh Kumar, Aashish Jha, Mohit Sahni, Richa Bhargava, Amit Chawla, Chandra, R.; Sanjeev Kumar, Chaubey, S. Effect of Annealing Temperature on the Physical Properties of Zn-ferrite Nanoparticles. J. *Supercond. Nov. Magn.* **2014**, *27*, 821-826.

[29] Yan Xu, Yantian Liang, Lijuan Jiang, HuaruiWu, Hongzhi Zhao, Desheng Xue. Preparation and Magnetic Properties of $ZnFe_2O_4$ Nanotubes. *J. Nanomater.* **2011**, 5.

[30] Shenoy, S. D.; Joy, P. A.; Anantharaman, M. R. Effect of mechanical milling on the structural, magnetic and dielectric properties of coprecipitated ultrafine zinc ferrite. *J. Magn. Magn. Mater.* **2004**, *269*, 217-226.

[31] Atif, M.; Hasanain, S. K.; Nadeem, M. Magnetization of sol–gel prepared zinc ferrite nanoparticles, Effects of inversion and particle size. *Solid State Commun*, **2006**, *138*, 416-421

The authors declare no conflict of interest